Engineering Structures 134 (2017) 303–316

Contents lists available at ScienceDirect

Engineering Structures

journal homepage: www.elsevier.com/locate/engstruct

Seismic reliability of legged wine storage tanks retrofitted by means of a seismic isolation device

J.I. Colombo *, J.L. Almazán

Department of Structural and Geotechnical Engineering, Pontificia Universidad Católica de Chile, Vicuña Mackenna, 4860 Santiago, Chile

ARTICLE INFO

Article history:
Received 15 August 2016
Revised 28 December 2016
Accepted 29 December 2016

Keywords:
Seismic isolation
Seismic reliability analysis
Wine storage tanks
Fragility curves

ABSTRACT

Due to the booming of the winery industry in some seismic countries such as, the U.S, Italy, New Zealand, Chile and Argentina, the seismic protection of wine storage tanks may be of a practical importance. Wine storage tanks are classified in two major groups: continuously supported tanks and legged tanks. Previous research has described the seismic reliability of continuously-supported tanks, with and without seismic protection devices. Conversely, the seismic reliability of legged wine tanks has not been reported. Therefore, in this study, the seismic reliabilities of two typical stainless steel legged wine storage tanks (one of 3000 L capacity and one of 17,100 L capacity), used for fermentation and wine storage, in original and updated states are assessed by means of simulation. For the updated state, a non-linear isolation system for seismic isolation of legged wine tanks is used. The effect of the isolation system was numerically estimated by performing a group of non-linear time history analyses for each tank. Each non-linear time history analysis was obtained by means of a mathematical model. A set of different seismic ground motions was used for the purpose of obtaining robust results in the reliability analysis. Finally, the seismic reliability analysis shows that, for steel legged wine storage tanks, the effect of the isolation system would reduce the limit state probability in the order of 90%.

1. Introduction

Liquid storage tanks are used in many different civil engineering applications and industrial facilities. Some of these applications are the storage of liquids such as water, wine, oil, nitrogen, high-pressure gas, petroleum, etc. Almost every major earthquake around the world has affected many of these tanks. For instance, several reports provide evidence of failure and extensive damage in liquid storage tanks such as during the 1960 earthquake in Chile [1], the 1964 earthquake in Alaska [2], the 1977 earthquake in San Juan, Argentina [3], the 1979 Imperial County earthquake [4], the 1980 Livermore earthquake [5], the 1983 Coalinga earthquake [6], and the 1994 Northridge earthquake (all in California) [7], the 2001 Bhuj earthquake in India [8], and the 2010 earthquake again in Chile [9]. Therefore, the poor seismic reliability of these structures is evident.

Considerable economic losses and environmental hazards have been caused by the loss of contents of these tanks [10,11]. The most common types of damage observed in liquid storage tanks are: damage to the piping connections caused by large base uplifts, damage to the roof caused by the sloshing of the free liquid surface, buckling of the tank walls caused by the high compressive stress, buckling of the tank legs caused by large axial loads coupled with lateral loads, failure of the anchorage system caused by the high overturning moment transmitted to the base, penetration of the tank wall with anchor bolts caused by the previous failure of the anchorage system and damage to the shell-base connection caused by the plastic rotation of the base plate. Among these causes, the failures that are responsible for a large or total loss of the liquids contained in storage tanks are buckling of the tank legs and rupture of the shell-base connection (see Fig. 1).

Due to the booming wine industry in some seismic countries such as the US, Italy, New Zealand, Chile and Argentina among others, seismic protection of wine storage tanks in the face of earthquake hazards is of paramount economic importance. However, as stainless steel wine tanks were not in use when the 1985 earthquake occurred in Chile [10], local evidence of seismic behaviour of these kinds of structures is limited to the recent earthquake in central Chile in 2010. Consequently, there is little information available on seismic hazards in metallic wine storage tanks. It is important to note that at present steel tanks represent 80% of the country's wine storage capacity [11].

Steel wine storage tanks are classified in two major groups: continuously supported tanks and legged tanks (see Fig. 2). Several

* Corresponding author.
E-mail address: jicolombo@uc.cl (J.I. Colombo).

http://dx.doi.org/10.1016/j.engstruct.2016.12.058
0141-0296/

Fig. 1. Common failures in steel wine storage tanks that imply loss of the liquid content: (a) buckling of the tank legs and (b) rupture of the shell-base connection.

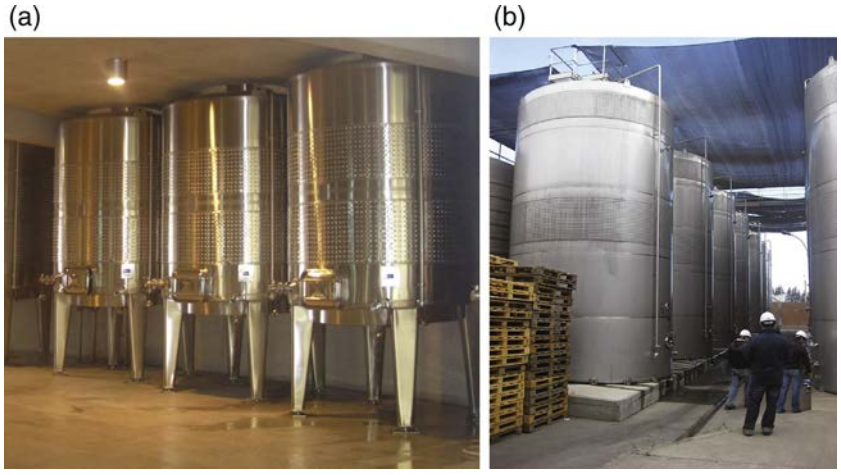

Fig. 2. Different foundation types for wine storage tanks: (a) legged tanks and (b) continuously supported tanks.

damages have been reported for both types of tanks. For instance, in the past 2010 earthquake in Chile the losses reached approximately 125 million litres of wine (250 million U.S. dollars) representing 12.5% of production in 2009 [11]. The earthquake struck a week before the start of the harvest, when only 50% of storage capacity was in use. This indicates that more than 25% of tanks with wine lost all or part of their content.

Recently numerous studies have been carried out in this field in order to improve seismic behaviour and to reduce the risk of damage or failure of liquid storage tanks [12,13]. In these studies two major alternatives are presented: seismic isolation and external energy dissipation. Some examples of seismic protection in liquid storage tanks using isolation systems are given by Shrimali and Jangid [14], Cho et al. [15], and Almazán et al. [10]. Similarly, examples of seismic protection in liquid storage tanks using external energy dissipation devices are published by Maleki and Ziyaefar [16,17], Pirner and Urushadze [18], Liu and Lin [19], Malhotra [20], Curadelli [21], Ormeño et al. [22] and Colombo and Almazán [23]. However, only a few works have been found in the technical literature concerning the seismic performance and protection of legged tanks. For instance, Almazán et al. [10] investigated numerically, with a deterministic approach, the seismic response of a typical legged tank equipped with seismic isolation devices in the bottom of its legs.

Probabilistic seismic risk analysis is one of the best tools for measuring the seismic performance of a structural system due to uncertainties related to structural performance and, predominantly, to excitation, [21,23–30]. Therefore, probabilistic seismic risk analysis has received increasing attention in the last two decades; however, previous work on probabilistic seismic risk analysis for liquid storage tanks is scarce. Only some recent investigations have presented a probabilistic seismic risk analysis for a few kinds of storage tanks; for instance, such risk analysis was published by Curadelli in order to assess the effectiveness of a specific retrofit on spherical storage tanks [21]. Similarly, a probabilistic seismic risk analysis was reported by Colombo and Almazán [23] in order to measure the effectiveness of a specific energy dissipation system on continuously supported wine storage tanks. It would appear earlier seismic reliability analyses for measuring the effect of any seismic improvement in legged cylindrical tanks have not been reported in the literature, i.e. only deterministic approaches have been shown in previous works. Additionally, it is important to remark that some recent studies have been carried out in order to evaluate the seismic reliability of structures isolated by friction pendulum devices [30,31].

Consequently, with the premise that the most appropriate approach for measuring the effect of any seismic protection system in structures under seismic excitation is a seismic risk analysis or reliability analysis [24], in this work the seismic reliability of two typical legged steel wine storage tanks – one of 3000 L capacity and one of 17,100 L capacity – with and without a seismic isolation system was evaluated numerically. More precisely, with the purpose of evaluating the effectiveness of using a novel seismic isolation system in this structure, the probability of reaching the limit state of two typical legged steel wine storage tanks with and without a seismic isolation system was calculated and compared. The

seismic behaviour of each structure is examined by performing a set of non-linear dynamic analyses based on a mathematical model that takes the fluid-structure interaction and the non-linear behaviour of the isolation system into account [25]. The behaviour of the isolation system due to restitutive element, i.e. the force-displacement relationship, was established by means of an ANSYS model and the respective non-linear pushover analysis. The behaviour of the isolation system due to the frictional effect in the tank legs was taken account with a frictional model proposed by Constantinou et al. [33]. This frictional model is capable of accounting for: (i) multidirectional motion at Teflon-steel interface, (ii) velocity and pressure dependence of the friction coefficient, and (iii) static friction effects. However, for this investigation the velocity and pressure dependence of the friction coefficient was not considered. Several artificial ground motions were considered in the simulation study in order to obtain robust results. The artificial ground motions were based on ground motion from subduction earthquakes recorded in Chile. The structures with the novel seismic isolation system showed a significant increase in structural reliability, measured by means of the reduction of the limit state probability.

2. Wine-tank considered

Typical legged tanks used for wine storage and fermentation are shown in Fig 2a. When subjected to a strong seismic ground motion the structure may undergo several failure modes. The most significant failure modes are: buckling of the tank legs and failure of the anchorage bolts at the legs. Therefore, the purpose of this research is to avoid such failures modes using a new device for seismic isolation.

The considered systems are two typical stainless steel legged cylindrical tanks, one of small storage capacity and one of large storage capacity (Table 1). The small-capacity tank's characteristics were: capacity 3000 L, 4 legs, radius $R = 0.8$ m, wall height $Hw = 1.7$ m, length of the legs $Lg = 0.9$ m, and the thickness of the wall and the plate of the legs is 2 mm. Similarly, the large-capacity tank's characteristics were: capacity 17,100 L, 5 legs, radius $R = 1.65$ m, wall height $Hw = 2.25$ m, length of the legs $Lg = 1.05$ m and the thickness of the wall and the plate of the legs is 2.5 mm. The material properties for both tanks were the same. The Young modulus of elasticity and the yielding stress of the tank material were 193 GPa and 310 MPa, respectively. The Poisson ratio was 0.3. The liquid content was wine with a density of 1000 kg/m^3 [11]. The legs of the tanks were resting on a rigid surface. The foundation where the tanks rested was excited by a tri-directional ground motion $\ddot{x}_{gx}(t)$, $\ddot{x}_{gy}(t)$ and $\ddot{x}_{gz}(t)$.

Two different configurations were analysed for each tank. The first configuration was the tank without the isolation system, in which the tank was just anchored to the foundation. The second configuration was the tank with the isolation system. In the latter configuration the legs of the tank were resting on a rigid surface, and were able to slide on that surface with the corresponding friction coefficient, μ. Two different values of friction coefficient were evaluated: 0.08 and 0.15. These values are the lowest and highest limit commonly observed for sliding coefficient of friction between Teflon-steel interfaces [33]. Additionally, in this latter configuration, the tank had a multi-spring central leg, which was the restitutive element of the isolation system (see Fig. 3). This multi-spring central leg was anchored to the tank base and the ground foundation.

Table 1
Characteristics of the small-capacity and large-capacity tanks.

	Small-capacity tank	Large-capacity tank
Capacity (l)	3000	17,100
Number of legs	4	5
Radius (m)	0.8	1.65
Wall height (m)	1.7	2.25
Length of the legs (m)	0.9	1.05
Thickness (mm)	2	2.5

3. Wine-tank model

In order to establish the main dynamic behaviour of the wine tanks a simplified mathematical model was used, which is shown in Fig. 4. The hydrodynamic pressures and forces in the tank can be expressed as the sum of two components. The first component is impulsive, representing the effect of the part of the liquid that moves in synchronism with the tank wall as a rigid body. The second component is convective, representing the effect of the part of the liquid that presents a sloshing motion. However, as the wine storage tanks were completely filled, sloshing was not possible. The completely filled condition is the normal condition for wine storage tanks [11]. Therefore, in this model only the impulsive component was considered. The values of the impulsive mode for the small-capacity tank were: $m_i = 2376$ kg, $h_i = 0.84$ m, $f_i = \omega_i/2\pi = 59.45$ Hz, $\zeta_i = 2\%$; similarly, the values of this mode for large-capacity tank were: $m_i = 10{,}602$ kg, $h_i = 1.01$ m, $f_i = \omega_i/2\pi = 36.64$ Hz, $\zeta_i = 2\%$, where m_i is the impulsive mass, ω_i is the natural frequency of the fixed-based impulsive component, ζ_i is its damping ratio, and h_i is the height of the resultant of the hydrodynamic wall pressures due to the impulsive component. These modal parameters of the impulsive mode of each tank were obtained from results published by Veletsos and Tang [32] and Veletsos et al. [34]. It is worth mentioning that this simplified mathematical model was proposed by Veletsos and Tang [32] and Veletsos et al. [34] for dynamic analysis of continuously supported tanks.

The isolation system had two main characteristics: energy dissipation and the restitutive element. Energy dissipation was a consequence of the sliding of the tank legs over the rigid surface. Two different values of the friction coefficient μ were considered: 0.08 and 0.15. As mentioned above, these values are the lowest and highest limit commonly observed for sliding coefficient of friction between Teflon-steel interfaces [33]. The restitutive element is a multi-spring central leg, which had a linear force-displacement relationship. In addition, it should be noted that the multi-spring central leg did not receive weight load from the tank, i.e. the weight of the tank was resisted by the original tank legs.

4. The base isolation system

Base isolation systems are one of the most efficient mechanisms available for seismic protection. The first applications of base isolation system to afford seismic protection to liquid storage tanks are attributed to Chalhoub and Kelly [35]. For this investigation, the isolation system consisted of one multi-spring central leg, acting as a restitutive element, and one slide bearing below each original tank leg, i.e. each original tank leg was able to slide with a friction coefficient μ. Due to the simplicity of the construction and the common use of spring as restitutive element, compression springs were used for the central leg. Moreover, the springs used at the bottom and the top of the central leg acted as spherical ball joints as well, i.e. the pattern in which the springs were used allows the tank to move horizontally in any direction.

The multi-spring central leg for the small-capacity tank was made with five springs, two big square plates, two small square plates and one tube. The side length of the big plates and the small plates were 50 cm and 27 cm, respectively. The thickness of these plates was 1 cm. The dimensions of the tube were: internal

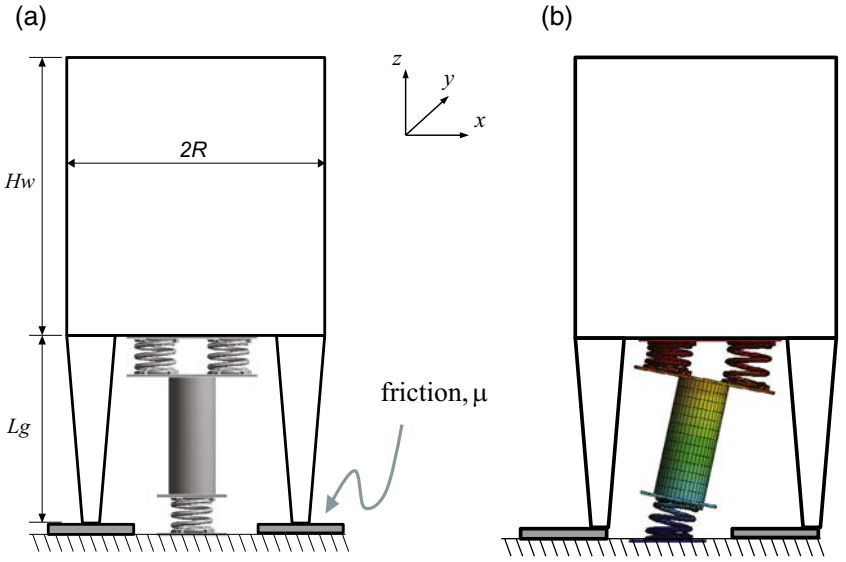

Fig. 3. Legged storage tank with the multi-spring central leg: (a) undeformed position and (b) deformed position.

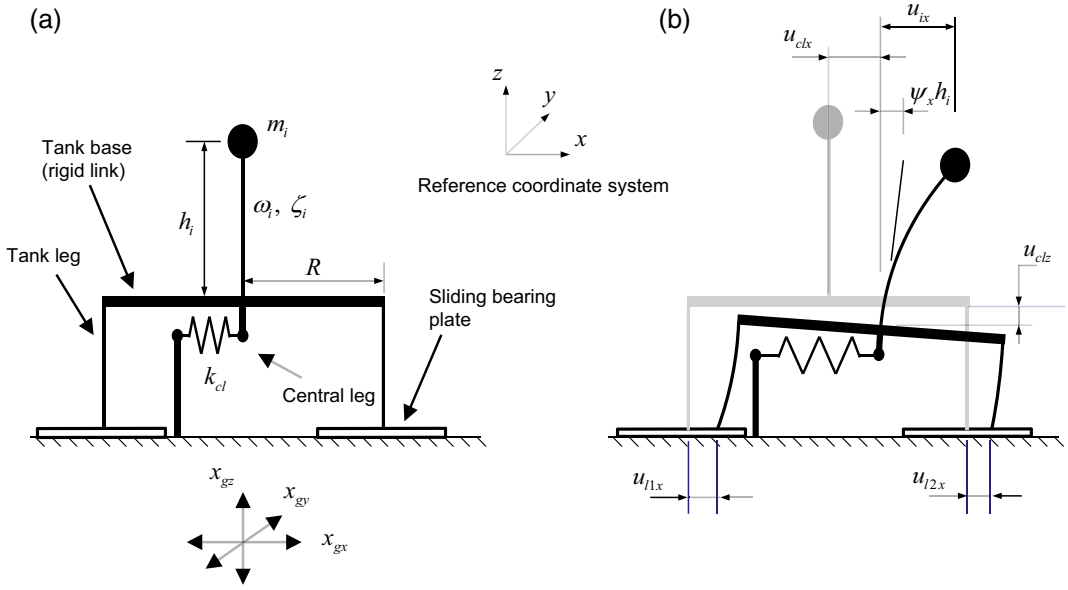

Fig. 4. Model of wine-tank-isolation system shown in Fig 3. (a) undeformed position and (b) deformed position.

diameter $\phi_i = 16$ cm, external diameter $\phi_e = 18$ cm, and length $l = 44.6$ cm. The dimensions of the springs were: free length $l_s = 13.7$ cm, wire diameter $d_w = 1.8$ cm, pitch $p = 3.7$ cm and external diameter $\phi_{es} = 16.2$ cm. These dimensions were used because they are rather common in the manufacturing the springs (e.g., suspension springs in vehicles). Similarly, the multi-spring central leg for the large-capacity tank was made with twelve springs, four square plates and one tube. The side length of the plates was 80 cm. The thickness of these plates was 1 cm. The dimensions of the tube were: internal diameter $\phi_i = 18$ cm, external diameter $\phi_e = 20$ cm, and length $l = 66$ cm. The dimensions of the springs were the same that the springs used in the multi-spring central leg for the small-capacity tank. These springs were used to connect the plates as is shown in Fig. 5. The considered material of the springs was SAE 9254 steel which is also widely used in the manufacture of springs. The central legs had the linear approximation for the lateral force-displacement relationship shown in Fig. 6. This relationship was obtained by the method described in the section below. It is important to remark that the number and configuration of the springs in the central legs were selected due to: (1) its easy manufacturing and (2) an esthetical aspect, namely hide most of the springs just below the base tank.

Additionally, it is important to remark that, with the respective lateral stiffness of each multi-spring central leg, the fundamental period of the respective isolated tank is approximately 2 s. In this context, it is worth mentioning that this is a novel approach to use these types of springs, i.e. using the flexural, shear and axial stiffnesses of compression springs. Some other options for realizing the restitutive element can be: (i) an auxiliary structure connected to the roof of the tank (Fig. 7(b)); (ii) a central-leg with a traditional rubber isolator on the top of the leg (Fig. 7c).

Finally, it is also worth mentioning that legged wine storage tanks have usually a stiffener ring that connects the top of the legs with the base of the tanks. This stiffener ring is one of the robust

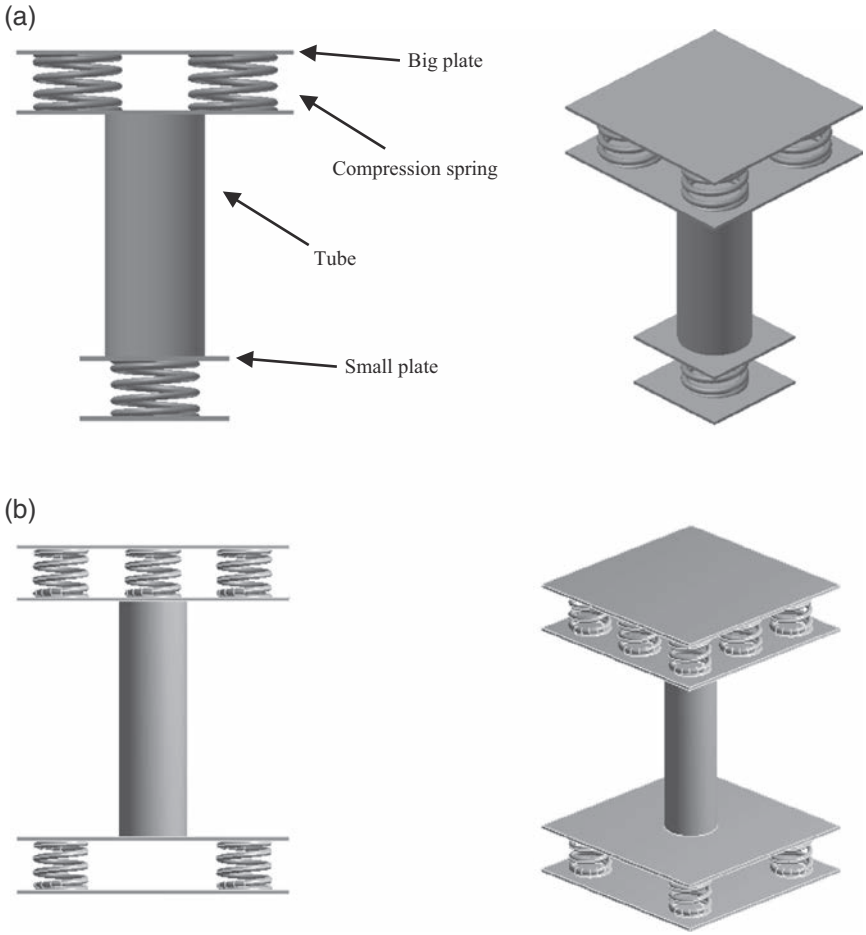

Fig. 5. Multi-spring central leg of (a) the 3000 L tank and (b) the 17,100 L tank: elevation and isometric views.

parts of the tank, and is the most suitable place to connect the restitutive element (see Fig. 8).

5. Multi-spring central leg model

In order to establish the force-displacement relationship of the multi-spring central leg, a 3D finite element model was used. This model was developed in ANSYS, and the force-displacement relationship was carried out with the aid of non-linear static pushover analysis. The stress-strain relation was determined by means of a bilinear isotropic hardening model, where the material parameters of the stress-strain relation for the plates and the tube were the same as those indicated in Section 2 and the tangent modulus was 1.8 GPa. However, the material used for the springs was SAE 9254 steel which had a yielding stress of 1470 MPa. The device was discretized using a 3-D 20-node solid element exhibiting a quadratic displacement behaviour (SOLID186). This element has three degrees of freedom per node (i.e. translation in the x, y and z directions of the nodal) and makes it possible to perform a non-linear analysis. Large displacement and deformation effects, such as large deflection, large rotation and large strain, were accounted for by using the non-linear geometry option in ANSYS.

Horizontal rollers located above the top plate were used to simulate the surrounding tank structure. These rollers kept the top plate horizontal during the lateral displacement of the tank. The bottom plate was fixed to the foundation. For brevity only the scheme of the multi-spring central leg of the small-capacity tank is shown in Fig. 9.

5.1. Pushover analysis

Non-linear static pushover analysis for the multi-spring central legs was carried out (displacement control analysis) using the respective multi-spring central leg model described above. Horizontal displacement history was applied to the top plate following a ramp-shaped function, i.e. linear and monotonic increasing. The horizontal displacement was raised up to 15 cm. This value was the maximum desirable displacement in order to maintain the safety of the surrounding structures, piping connections and the compression springs. The displacement step was equal to 15 mm.

The Von Mises stress distribution of the structure subjected to horizontal displacement was calculated for each displacement step. For the multi-spring central leg of the small-capacity tank, the maximum Von Mises stress value in the springs was 1168 MPa (Fig. 10a). In the other parts of the central leg, i.e. the tube and the plates, the maximum Von Mises stress value was 137 MPa. In both cases, the structure is shown in the deformed configuration (Fig. 10). Similarly, for the multi-spring central leg of the large-capacity tank, the maximum Von Mises stress value were 1250 MPa and 280 MPa in the springs and the plates, respectively (Fig. 11). As expected, the stresses were highly concentrated at some coils of the springs, where the maximum effective stress reached 1250 MPa. Hence, comparing these maximum stress values with the yielding stresses indicated in Sections 2 and 5, i.e. 310 MPa for steel of the plates and the tube and 1470 MPa for SAE 9254 steel used in the springs, it can be concluded that the multi-spring central legs will remain without failure. As mentioned

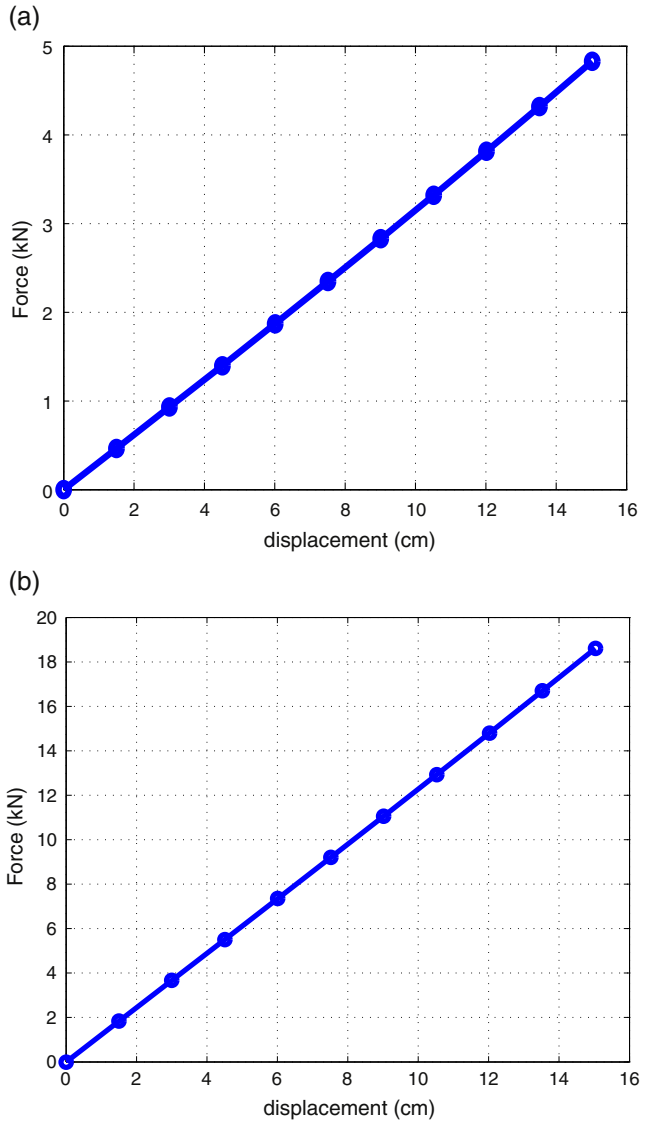

Fig. 6. Force-displacement relationship for the multi-spring central leg of the: (a) 3000 L tank and (b) 17,100 L tank.

above, the lateral force-displacement relationship of both central legs is shown in Fig. 6.

6. Solution method for the non-linear time history analysis

The governing equations of motion of the masses m_i in Fig. 4, in x- and y-directions, are

$$m_i\ddot{u}_{ix} + c_i(\dot{u}_{ix} - h_i\dot{\psi}_x) + k_i(u_{ix} - h_i\psi_x) = -m_i(\ddot{u}_{clx} + \ddot{x}_{gx}) \quad (1)$$

$$m_i\ddot{u}_{iy} + c_i(\dot{u}_{iy} - h_i\dot{\psi}_y) + k_i(u_{iy} - h_i\psi_y) = -m_i(\ddot{u}_{cly} + \ddot{x}_{gy}) \quad (2)$$

where u_{ix} and u_{iy} are the displacement of the mass m_i relative to the centre of the base tank in x- and y-directions, respectively; ψ_x and ψ_y are the base rotation in x- and y-directions, respectively; and u_{clx}, u_{cly} and u_{clz} are the displacement of the centre of the base tank relative to ground in the x-, y- and z-directions, respectively; an overdot denotes differentiation with respect to time. Additionally, the governing equations of motion of the structure below the base tank, i.e. the frame structure representing the legs and the isolation system, are expressed in the matrix form, for the small-capacity tank, as

$$[K_s]\{u_s\} + \{F_i\} + \{F_p\} = \{0\} \quad (3)$$

$$u_s = [u_{clx} \quad \psi_x u_{cly} \quad \psi_y u_{clz} \quad u_{l1x} \quad u_{l2x} \quad u_{l3x} \quad u_{l4x} \quad u_{l1y} \quad u_{l2y} \quad u_{l3y} \quad u_{l4y} \quad u_{l1z} \quad u_{l2z} \quad u_{l3z} \quad u_{l4z}]^T \quad (4)$$

$$F_i = [-m_i(\ddot{u}_{clx} + \ddot{u}_{ix} + \ddot{x}_{gx}) \quad -m_i h_i(\ddot{u}_{clx} + \ddot{u}_{ix} + \ddot{x}_{gx}) \quad -m_i(\ddot{u}_{cly} + \ddot{u}_{iy} + \ddot{x}_{gy}) \quad \ldots \quad -m_i h_i(\ddot{u}_{cly} + \ddot{u}_{iy} + \ddot{x}_{gy}) \quad -m_l(g + \ddot{u}_{clz} + \ddot{x}_{gz}) \quad 0 \quad 0 \quad 0 \quad 0 \quad 0 \quad 0 \quad 0 \quad 0 \quad 0 \quad 0]^T \quad (5)$$

$$F_p = [0 \quad 0 \quad 0 \quad 0 \quad 0 \quad F_{1x} \quad F_{2x} \quad F_{3x} \quad F_{4x} \quad F_{1y} \quad F_{2y} \quad F_{3y} \quad F_{4y} \quad N_1 \quad N_1 \quad N_3 \quad N_4]^T \quad (6)$$

where K_s is the stiffness matrix of the structure below the base tank, i.e. the original tank legs and the multi-spring central leg; F_i is the transmitted loads vector of the impulsive mass to the structure; F_p is the force vector due to the interaction between the bottom of the original tank legs and the sliding bearing plates, i.e. the vector of the friction and normal forces; F_{1x}, F_{2x}, F_{3x} and F_{4x} are the friction forces in x-direction at each one of the four original tank legs of the tank; F_{1y}, F_{2y}, F_{3y} and F_{4y} are the friction forces in y-direction at each one of the four original legs of the tank; N_1, N_2, N_3 and N_4 are the

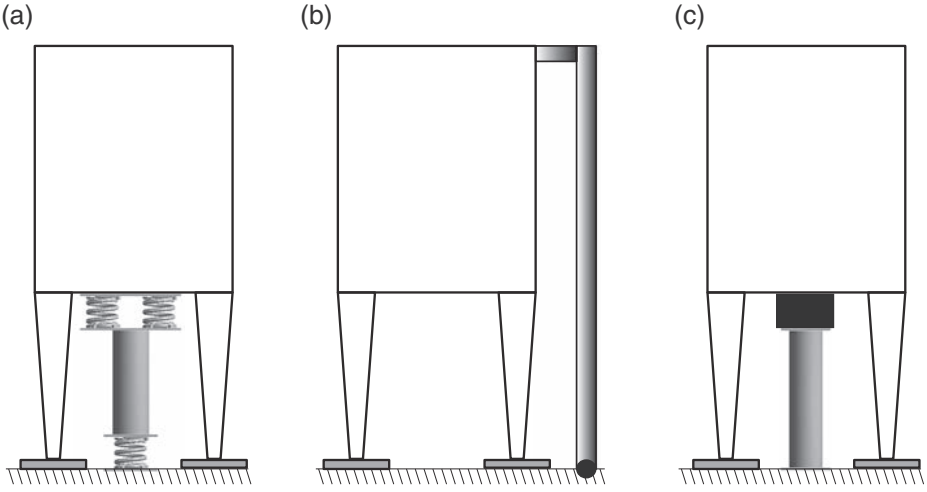

Fig. 7. Some possible options for realizing the restitutive element: (a) a multi-spring central leg, (b) an auxiliary structure connected to the tank, and (c) a central leg with a traditional rubber isolator.

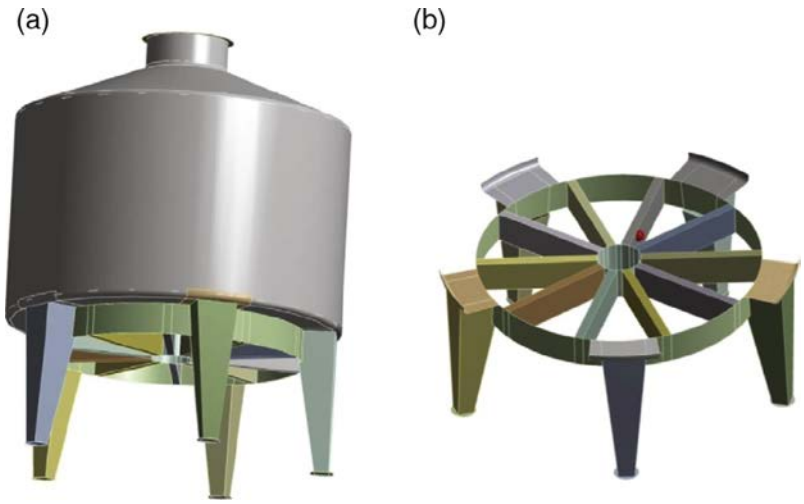

Fig. 8. Schematic views of a typical legged wine storage tank: (a) the entire tank and (b) the stiffener ring of the tank [11].

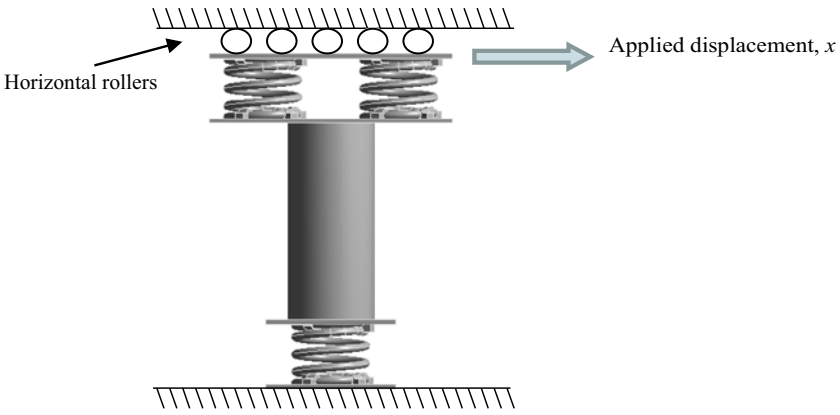

Fig. 9. Multi-spring central leg boundary conditions and applied loading.

normal forces in z-direction at each one of the four original legs of the tank; u_s is the displacement vector; u_{l1x}, u_{l2x}, u_{l3x} and u_{l4x} are the displacements in x-direction of the bottom of each one of the four original tank legs relative to ground; u_{l1y}, u_{l2y}, u_{l3y} and u_{l4y} are the displacements in y-direction of the bottom of each one of the four tank legs relative to ground; and u_{l1z}, u_{l2z}, u_{l3z} and u_{l4z} are the displacements in z-direction of the bottom of each one of the four tank legs relative to ground. It is important to remark that the z-direction displacements at the bottom of each one of the tank legs were considered in order to estimate the normal force that is required by the frictional model proposed by Constantinou et al. [33]. More precisely, each tank leg was resting on a compression-only spring which was capable of estimating the normal force and taking into account for contact and non-contact conditions between the tank legs and the ground. Geometric nonlinearities were not taken into account in the stiffness matrix K_s. For the tank with five legs, i.e. the large-capacity tank, it was added one more leg in the Eqs. (4)–(6). Finally, Eqs. (1)–(3) were integrated in time using standards ODE solvers in MATLAB [36].

It is worth mentioning that the stiffness matrix K_s was built considering four frame elements connected to a rigid circular plate (see Fig. 4). Each frame element has one end fixed to the rigid circular plate (i.e. the tank base) and the other end with a node with three degrees of freedom (i.e. translation in the x, y and z directions of the nodal). The rigid circular plate has one node at its centre with five degrees of freedom (i.e. translation in the x, y and z directions of the nodal and rotation in the x and y directions of the nodal). Additionally, dissipative terms associated to the hysteretic behaviour of the tank were considered only in Eqs. (1) and (2), i.e. only dissipative terms related with the impulsive component were considered.

7. Structural reliability

The procedure for evaluating the effectiveness of the seismic isolation system through a reliability analysis of legged supported tanks was essentially as follows: (1) a set of seismic ground motions was obtained and normalized by the peak ground acceleration (PGA), (2) fragility curves were constructed by simulation, counting the relative number of times that the limit state of the structure is achieved for each PGA level, and (3) the limit state probability was estimated with the aid of fragility curves in conjunction with the seismic hazard at the structure site. The limit state probability for an N-year period in seismic risk assessment was estimated using the expression

$$P_F = \sum_x P[C = 1|Q = x]P[Q = x] \tag{7}$$

where C is the random variable that represents the limit state of the structure and Q is related to the ground motion intensity level, $P[C = 1|Q = x]$ is the conditional probability of reaching the limit state given the occurrence of a seismic ground motion with a specific value of intensity x, and $P[Q = x]$ is the probability that this seismic

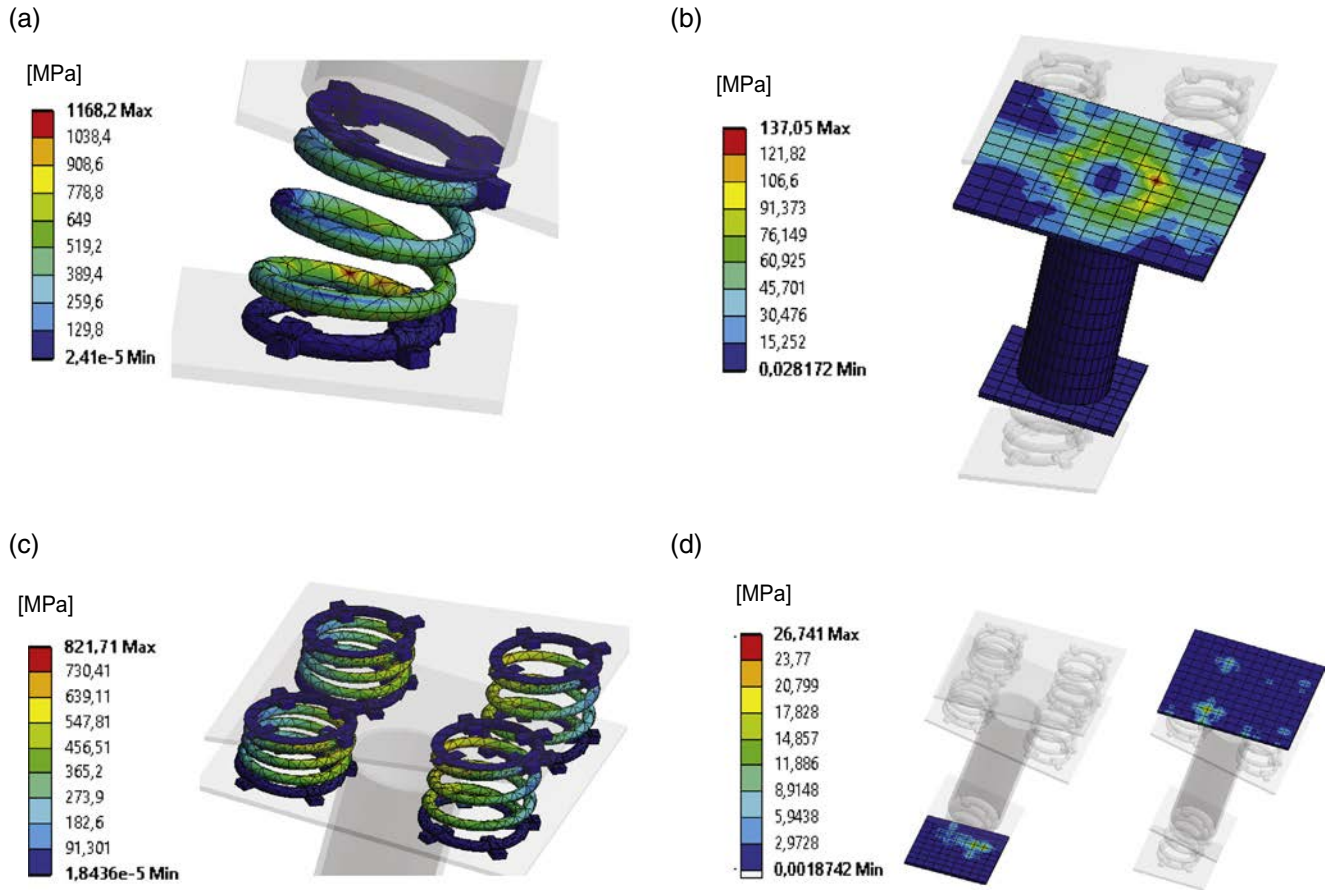

Fig. 10. Von Mises stress distribution (in MPa) of the central leg model for the 3000 L tank subjected to horizontal displacement applied to the top plate at maximum condition for: (a) the bottom spring; (b) the tube and centre plates; (c) the top springs; and (d) the top and bottom plates.

ground motion intensity exceeds the specific level x during a given time period.

This procedure was carried out on the tanks and analysed for each of the two different configurations mentioned in Section 2 and the results were compared in order to assess the effectiveness of the seismic isolation system.

7.1. Seismic ground excitation

A fundamental aspect of developing a reliability analysis is that a set of ground motions is required (step (1) of the procedure above), for which artificial acceleration time histories or actual earthquake records may be used [24]. In the present investigation, a set of twenty-two artificial seismic ground motions in accordance with the Chilean code spectrum was assumed [37]. More precisely, an elastic design spectrum for 5% damping and a soil classified as type II of the Chilean code was considered. Near-fault effects were not taken into account because the fault rupture process at the structure site was not related to a near-source fault. The considered seismic ground motions were non-stationary. Each record was converted thorough the Fourier transform to the frequency domain and scaled to match the intensity of the spectrum. Then, the signal was reverted and the result was a spectrum–compatible record [38]. Each record was normalized to twenty-four specified levels of peak ground accelerations. The total set of twenty-two artificial records, scaled to the twenty-four levels of PGA, was the seismic ground excitation ensemble considered for the probabilistic analysis. These twenty-four levels of PGA were selected in order to consider a wide range of PGA with a small increment step, i.e. the PGA ranges from 1 m/s^2 to 12.25 m/s^2 with an increment step of 0.25 m/s^2. It is worth noting that different scaling procedures and different intensity measure are possible [39], such as *peak ground velocity* or *response-spectrum intensity* among others but it is not expected that the differences in seismic reliability will be affected by this choice. The PGA was used as intensity measure due to the fact that the seismic hazard curves are commonly reported in PGA (e.g., [21,23]).

7.2. The failure criterion and fragility model

The fragility curve is defined as the probability of reaching or exceeding the limit state for a particular value of the ground motion intensity. Consequently, to build the fragility curves (step (2) of the procedure above) a failure criterion for the analysed structures is required. Although numerous failure criteria have been proposed in the technical literature [40–44], for the current investigation it was decided that the limit state of damage in the tank occurred when any original leg of the tank reached the buckling condition or when the lateral displacement exceeded the maximum allowed displacement. Therefore, the limit state or failure was reached when

(a) in the anchored tank (i.e. the tank without the seismic isolation system), the axial and shear combined loads at any tank leg became equal to or greater than the allowed combined load value;
(b) in the anchored tank (i.e. the tank without the seismic isolation system), the tension axial force at any tank leg became equal to or greater than the allowed tension axial force (i.e. 60 kN);

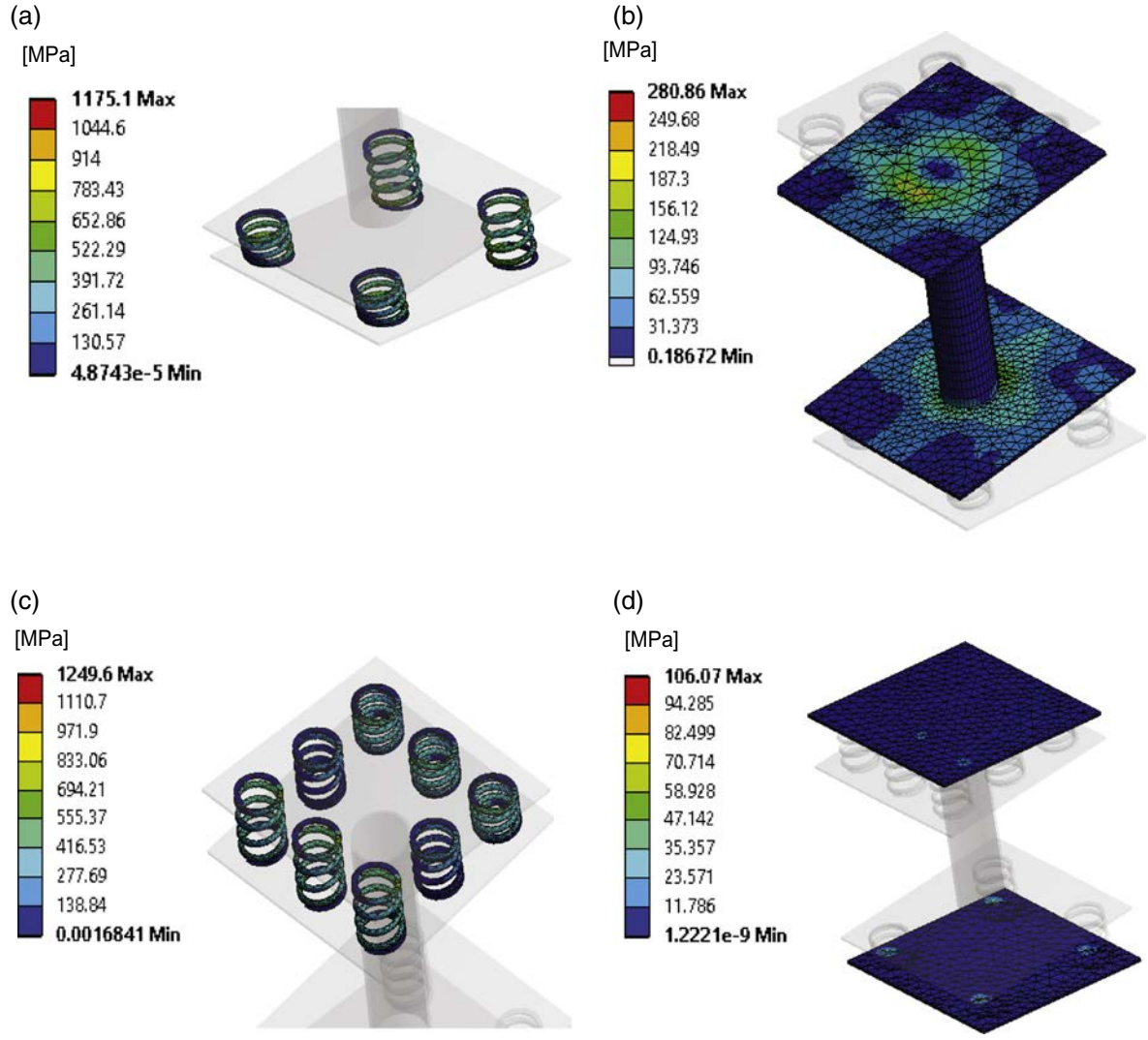

Fig. 11. Von Mises stress distribution (in MPa) of the central leg model for the 17,100 L tank subjected to horizontal displacement applied to the top plate at maximum condition for: (a) the bottom spring; (b) the tube and centre plates; (c) the top springs; and (d) the top and bottom plates.

(c) in the retrofitted tank (i.e. the tank with the seismic isolation system), the axial and shear combined loads at any tank leg became equal to or greater than the allowed combined load value;
(d) in the retrofitted tank, the lateral displacement of the central leg became equal to or greater 15 cm.

More precisely, the buckling condition of the tank legs was evaluated by the method described by Ashraf et al. [45], and also used by Gonzaléz et al. [11]. It is important to remark that this failure condition is a local buckling condition which occurs during the elastic behaviour of the tank legs.

It should be noted that, in order to achieve the aim of the present work, it is not necessary to define several failure criteria that rigorously quantify the damage level of the structure under seismic excitation. One damage state (failure or no failure) was considered to be sufficient as the objective of the present work was to compare the performances prior to and after the structural retrofit.

Therefore, it is possible to define a failure random variable C as

$$C\begin{cases}=1 \text{ if } (F_s,F_a) \geqslant (F_s,F_a)_{\text{lim}} \text{ or } F_t \geqslant F_{t\text{lim}} \text{ or } w \geqslant w_{\text{lim}} & \text{(failure)}\\ =0 \text{ otherwise} & \text{(no failure)}\end{cases} \quad (8)$$

where (F_s, F_a), F_t and w are the respective maximum values of the shear and axial combined forces at the tank legs, the tension axial force at the tank legs and lateral displacement at the central leg during a seismic event. Similarly, $(F_{s,} F_a)_{\text{lim}}$ are the values of the axial and shear combined forces that provoked the failure at the original tank legs; $F_{t\ \text{lim}}$ is the value of tension axial force that provoked the failure at the anchorage of the leg, and w_{lim} is considered as a conservative value of the lateral displacement that provoked the failure at the central leg. All these values were defined in (a), (b), (c) and (d) for each case.

After obtaining the set of seismic ground motions, the structural model and the failure criterion were defined, and the structural responses of the tanks for each anchorage system were calculated for each excitation sample by means of non-linear time history analysis. The conditional failure probability distribution was assessed counting the relative number of times the response reached the limit value for the combined axial and shear forces (for the cases defined in (a) and (c)), the limit value for the tension axial force (for the case defined in (b)) or the limit value for the lateral displacement of the central leg (for the case defined in (d)), which can be expressed as

$$P_C = P[C = 1|Q = x] \quad (9)$$

where C is the random variable that represents the limit state of the structure and Q is related to the ground motion intensity level, expressed in terms of the peak ground acceleration. Therefore, P_C is the probability of event $C = 1$ given a peak ground acceleration of x.

The fragility curves related to seismic analysis, and as functions of the peak ground acceleration, have a lognormal functional form given by (see e.g. [46–49])

$$P_C(x) = \phi\left[\frac{1}{\beta}\ln\left(\frac{x}{\mu}\right)\right] \tag{10}$$

where $\phi[\,]$ is the standard normal cumulative distribution function, μ is the median value of peak ground acceleration for which the connection reaches the 50th percentile of fragility, and β is the logarithmic standard deviation of the PGA for the limit state $C = 1$. These parameters are determined by fitting a lognormal function to the conditional failure probability distribution obtained from Eq. (9).

7.3. The seismic hazard model

In Eq. (7), the term $P[Q = x]$ represents the distribution of possible ground motion intensity levels determined as the derivative of the seismic hazard curve $H(x)$. This derivative of the seismic hazard is usually modelled using a complementary cumulative distribution function obtained from a seismic hazard analysis (SHA) of the site over a period of time. The hazard curve, in recent seismic risk analyses, has been described by a Type II distribution of largest values as (see e.g. [25])

$$H(x) = 1 - \exp\left[-\left(\frac{x}{u}\right)^{-k}\right] \tag{11}$$

where u and k are the scale and shape parameters of the distribution, respectively. More details on probabilistic seismic hazard analysis can be found in Lee et al. [50], Field [51], SSHAC [52] and McGuire [53].

7.4. Estimation of the limit state probability

The limit state probability, Eq. (7), can be estimated by convolving the fragility $P_C(x)$ with the derivative of the seismic hazard curve $H(x)$ as follows

$$P_F = \int_0^\infty P_C(x)\frac{dH(x)}{dx}dx \tag{12}$$

Assuming that only a relatively narrow range of x values in the integrand of Eq. (12) contributes significantly to P_F, the limit state probability can be approximated by (see e.g. [25,54])

$$P_F \approx H(\mu)\exp\left[\frac{(k\beta)^2}{2}\right] \tag{13}$$

Consequently, the limit state probability was estimated with the seismic hazard $H(x)$ and evaluated at the median fragility μ, and multiplied by a correction factor that takes into account the parameters related to the uncertainties associated with the ground motion intensity (measured by k) and the structural capacity (measured by β). It should be mentioned that the latter two parameters, k and β, were obtained by means of evaluation of the seismic hazard model and the fragility model, respectively. Typical values of k are in the range of approximately 1.5–2.5 in regions of moderate seismicity and 3–4 in highly seismic zones [55]. Similarly, the values of β vary between 0.15 and 0.25 depending on the structural performance level [56].

8. Discussion of results

The seismic fragility relations and the limit state probabilities for both legged wine storage tanks (small-capacity and large-capacity) with two different configurations were estimated using the procedure described in Section 7. The fragility points obtained from the simulation (Eq. (9)) were fitted with a lognormal function with 95% confidence for each configuration in both tanks, i.e. the small-capacity and large-capacity tanks with and without the isolation system (Figs. 12and 13, respectively).

A considerable increase in the capacity against failure of the structure was observed with the seismic isolation system (Figs. 12 and 13). For instance, in order for the small-capacity tank without the isolation system to reach the fifty percent probability of failure due to the buckling of the original tank legs, i.e. the median fragility, a peak ground acceleration of 4.05 m/s^2 was necessary. It is worth mentioning that, for the small-capacity tank without the isolation system, the first failure that occurred was the buckling of the tank legs. At the same time, for the tank with the isolation system with a friction coefficient $\mu = 0.08$, in order to reach the median fragility a PGA of 9.71 m/s^2 was required for the failure due to a large displacement of the central leg. The buckling failure was not reached at this configuration, i.e. isolated tank with a friction coefficient $\mu = 0.08$, for the range of PGA analysed. Similarly, for the tank with the isolation system with a friction coefficient $\mu = 0.15$, the PGA at the median fragility was as follows: 10.31 m/s^2 for buckling failure and 12.23 m/s^2 for the central leg failure (Fig. 12). As can be seen, the rise in the PGA that was required to reach the median fragility by using the isolation system represented an increase of 140% and 155% for a friction coefficient of $\mu = 0.08$ and $\mu = 0.15$, respectively (Table 2). As can be expected, the lower is the friction coefficient, the larger are the lateral displacements of the tank base; and the higher is the friction coefficient, the larger are the loads at the tank legs (Fig. 12). Therefore, the results in Table 2 shows that, for the small-capacity tank, a friction coefficient of $\mu = 0.15$ presented better result compared with a friction coefficient of $\mu = 0.08$. In other words, the small-capacity tank was more susceptible to the failure due to a large lateral displacement than to the buckling failure of the legs.

The large-capacity tank presented a similar behaviour (Fig. 13), where the PGA at the median fragility was as follows: 2.67 m/s^2 for the buckling failure in the tank without the isolation system, 10.22 m/s^2 for the buckling failure in the isolated tank with a friction coefficient $\mu = 0.08$, 9.66 m/s^2 for the large displacement failure in the isolated tank with a friction coefficient $\mu = 0.08$, and 6.87 m/s^2 for the buckling failure in the isolated tank with a friction coefficient $\mu = 0.15$ (Table 3). The large displacement failure in the isolated tank with a friction coefficient $\mu = 0.15$ was not reached for the range of PGA analysed. It is worth noting that, for the large-capacity tank, a friction coefficient of $\mu = 0.08$ presented better result compared with a friction coefficient of $\mu = 0.15$. This result shows the opposite result with those of the small-capacity tank (Table 2). In other words, the large-capacity tank was more susceptible to the buckling failure of the legs than to the failure due to a large lateral displacement.

This increase in the capacity against the failure of the tanks with the seismic isolation system was achieved due to (1) the increase in the energy dissipated as a result of the friction at the bottom of the legs, (2) the changes on the period of the dynamic response of the structure and (3) the fact that the maximum shear force at the tank legs was limited by the maximum frictional force. For instance, in order to compare the tanks with and without the seismic isolation system subjected to an earthquake with a mean recurrence interval of 475 years (approximately with a PGA of 3.7 m/s^2 in the region), the axial and shear forces of the most

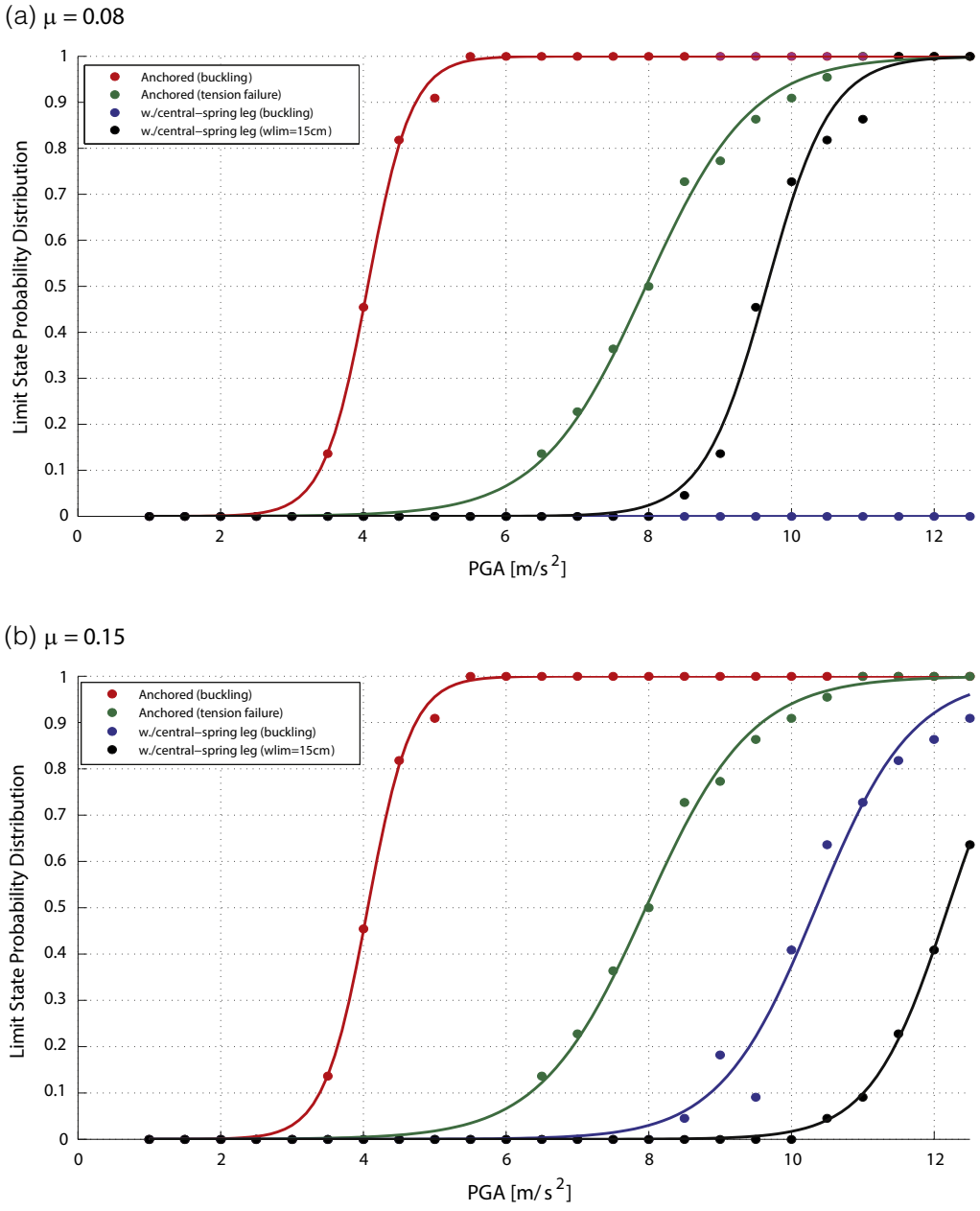

Fig. 12. Seismic fragility relations for the 3000 L tank with and without seismic isolation system: (a) with a friction coefficient μ = 0.08 and (b) with a friction coefficient μ = 0.15.

demanded leg of each tank are shown in Fig. 14. These results were obtained from the time history analysis of one ground motion record with the above PGA of the seismic ground motion ensemble. As can be seen, the legs of the tanks with the seismic isolation system presented shear and axial forces lower that the shear and axial forces on the legs of the tank without the seismic isolation system. Furthermore, Fig. 14 shows that the tanks without the seismic isolation system failed due to the buckling of the legs or tension axial force at the anchorage of the legs.

The seismic hazard curve $H(x)$, over a period of 100 years and obtained from the SHA based on the historical and instrumental data of the region is presented in Fig. 15. This seismic hazard curve is reported in the Chilean seismic code for a seismic zone classified as type 2 [37]. The parameters k and u of Eq. (11) were fitting with this seismic hazard curve. On a 100-year basis, the seismic hazard of the small-capacity tank with and without the isolation system, evaluated at the median fragilities (4.05 m/s^2, 9.71 m/s^2 and 10.31 m/s^2, respectively), came to the values 0.1637, 0.0176 and 0.0151, respectively. Multiplying these values by the exponential factor (see Eq. (13)) the limit state probabilities were 0.1718, 0.0180 and 0.0156, respectively (Table 2). Similarly, the seismic hazard of the large-capacity tank with and without the isolation system, evaluated at the median fragilities (2.67 m/s^2, 9.66 m/s^2 and 6.87 m/s^2, respectively), resulted in the values 0.4169, 0.0179 and 0.0433, respectively. Again, multiplying these values by the exponential factor (Eq. (13)) the respective limit state probabilities amounted to 0.4233, 0.0182 and 0.0451. Thus, the probability of reaching the limit state of the structure was reduced significantly in both tanks, i.e. by at least 90%, using the seismic isolation system.

The above results can also be interpreted as follows: An earthquake with a mean recurrence interval of 970 years (10% of being exceeded in 100 years) might be described approximately by a

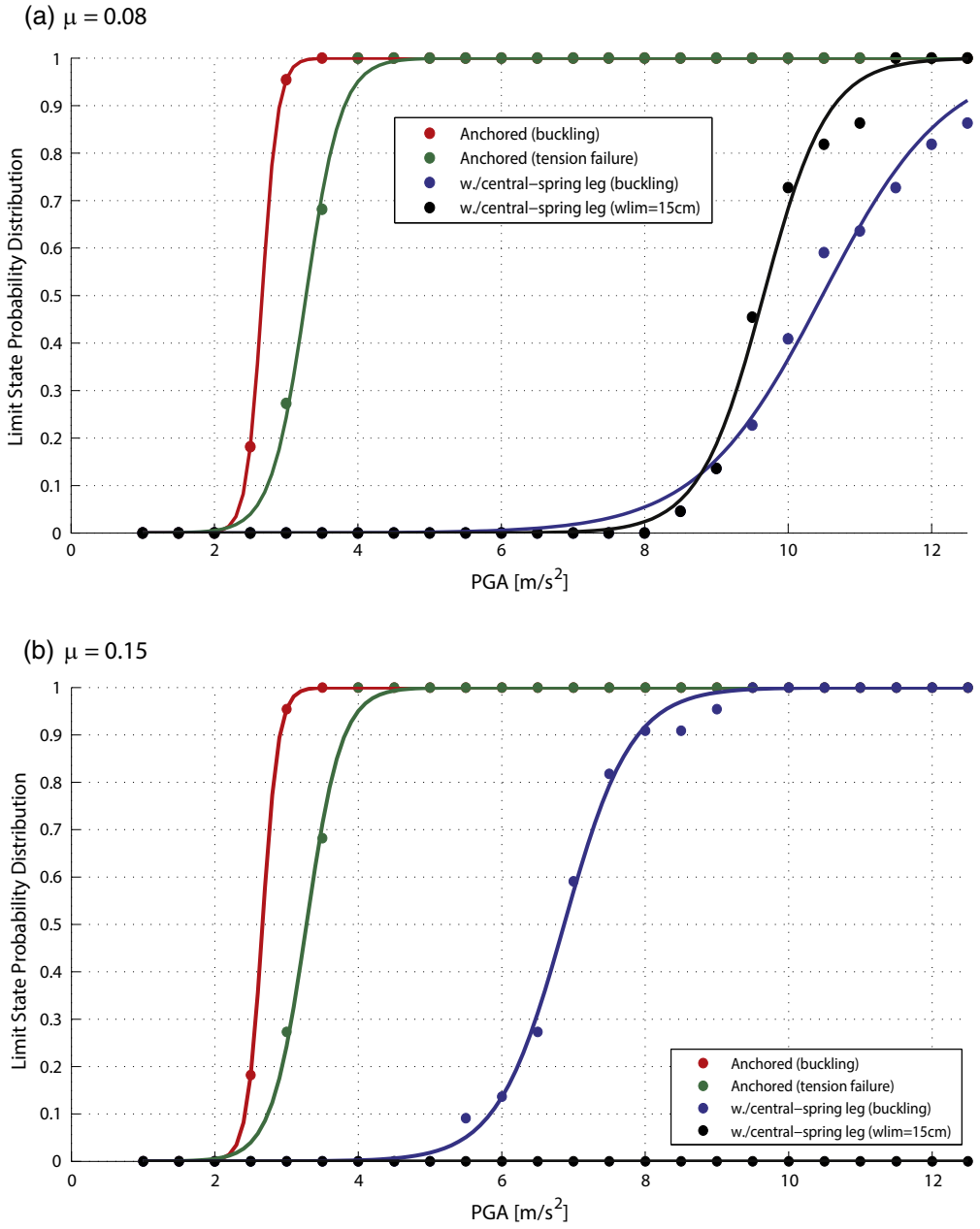

Fig. 13. Seismic fragility relations for the 17,100 L tank with and without seismic isolation system: (a) with a friction coefficient μ = 0.08 and (b) with a friction coefficient μ = 0.15.

Table 2
Limit state probability and PGA at median fragility of the 3000 L legged wine storage tank with and without a novel seismic isolation system (over a 100-year period).

	Without seismic isolation system	With seismic isolation system	
		μ = 0.08	μ = 0.15
Limit state probability	0.1718	0.0180	0.0156
PGA (m/s^2) at median fragility	4.05	9.71[a]	10.31[b]

[a] Failure due to a large displacement at the multi-spring central leg.
[b] Failure due to the buckling of a tank leg.

Table 3
Limit state probability and PGA at median fragility of the 17,100 L legged wine storage tank with and without a novel seismic isolation system (over a 100-year period).

	Without seismic isolation system	With seismic isolation system	
		μ = 0.08	μ = 0.15
Limit state probability	0.4233	0.0182	0.0451
PGA (m/s^2) at median fragility	2.67	9.66[a]	6.87[b]

[a] Failure due to a large displacement at multi-spring central leg.
[b] Failure due to the buckling of a tank leg.

PGA of 4.7 m/s^2 in the region (Fig. 15). At this ground motion intensity and for the tank without the isolation system, both the small-capacity and large-capacity tanks has over a 90% probability of reaching their limit states (Figs. 12 and 13, respectively) whereas at the same ground motion intensity, the retrofitted tanks with the isolation system has less than 1% probability of reaching its

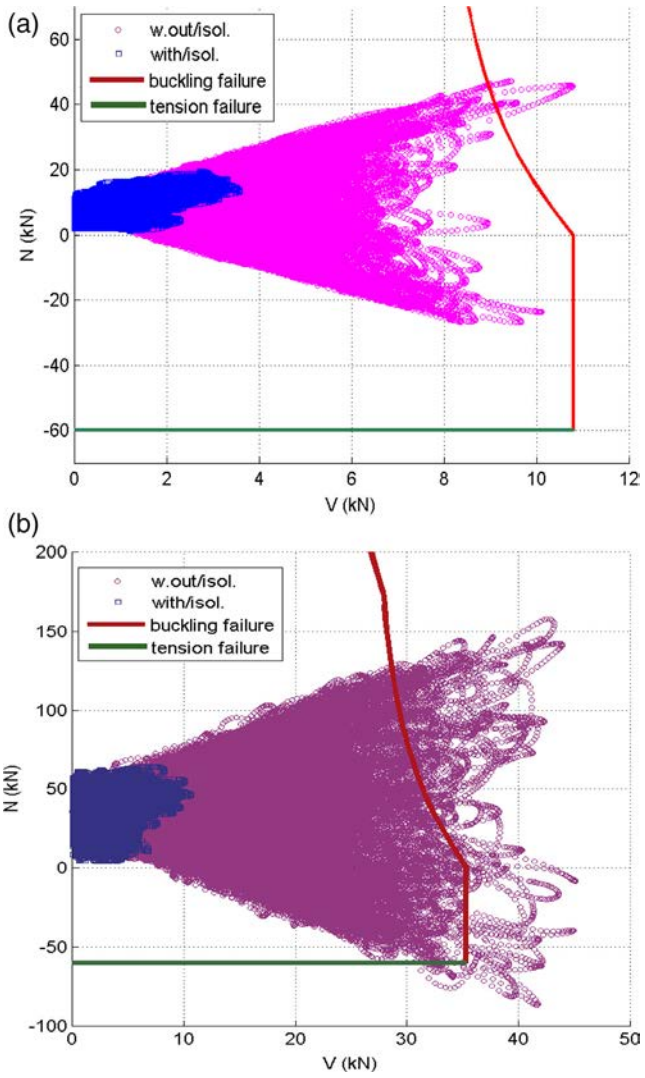

Fig. 14. Axial (N) and shear (V) combinations for the legs of the wine tanks: (a) 3000 L tank and (b) 17,100 L tank. Positive values of N correspond to compression forces.

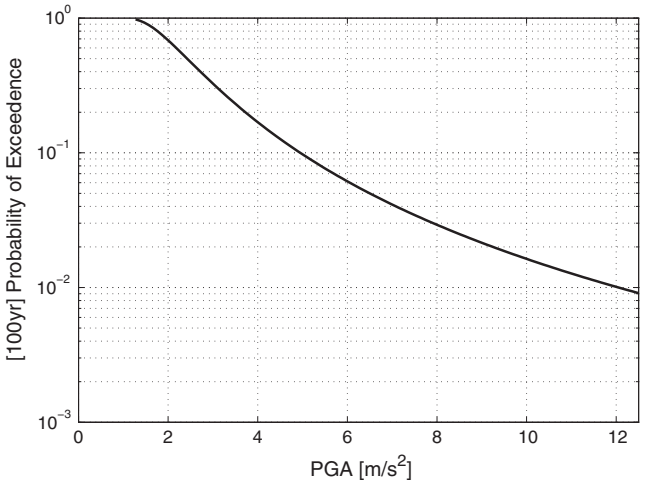

Fig. 15. Seismic hazard curve for a 100-year period.

limit state. As explained above, this significant reduction in the failure probability is a direct consequence of the increment in the amount of the dissipated energy, the change of period in which the tanks response dynamically and the limit on the maximum shear force transmitted to the tank legs.

It should be noted that the measuring of the effectiveness of the seismic isolation system installed on legged wine storage tanks presented here is different from the deterministic approaches shown in previous works, in which acceleration or displacement reductions are evaluated. The results presented in this investigation were obtained by a probabilistic method that offers a more reliable measure of the expected seismic performance because it considers the uncertainties related to structural behaviour and excitation. Finally, the robustness of the results presented in this study is one of the main advantages as the results are expressed in terms of risk reduction and not in terms of a particular acceleration or of displacement reductions.

Additionally, it is worth mentioning that the results herein presented can be extended for any of the above-mentioned options for realizing the restitutive element (see Section 4). However, the deformation limits of these other options should be estimated. Ongoing researches are developing restitutive elements made of rubber hinges, which work, principally, with their flexural stiffener.

9. Conclusions

The effectiveness of a seismic isolation system in two typical legged wine storage tanks (one of small storage capacity and one of large storage capacity) was assessed by means of the seismic reliability concept. The seismic reliability analysis of the storage tanks with and without the seismic isolation system was developed by simulation. For the tanks with the seismic isolation system, two different failure criteria were evaluated: (1) failure due to buckling of the tank legs, and (2) failure due to a large lateral displacement of the restitutive element. Similarly, for the tank without the seismic isolation system, two different failure criteria were evaluated: (1) failure due to buckling of the tank legs, and (2) failure due to a large tension axial force at the anchorage of the tank legs. The seismic reliability analysis showed that the seismic isolation system was very effective in reducing the probability of reaching the limit state of the structure by at least 90% in both the small-capacity and the large-capacity tank.

The following conclusions are based on the results presented in this work:

- The lowest seismic reliability condition of legged wine storage tanks is the anchored condition. The failure on this condition is due to the buckling of the tank legs.
- For anchorage legged wine storage tanks, the failure due to the buckling of the tank legs has a lower seismic reliability than the failure due to a large tension axial force at the anchorage of the legs.
- For legged wine storage tanks, large capacity storage tanks have a lower seismic reliability than small storage capacity tanks.

Acknowledgments

The authors wish to acknowledge the financial support provided by CONICYT-PCHA/Doctorado Nacional/2013-63130131 and the FONDECYT project number 1120937. In addition, the authors would like to thank the TPI America industry for the information about the dimensions of the legged wine storage tanks.

References

[1] Steinbrugge KV, Flores R. The Chilean earthquakes of May 1960: a structural engineering view point. Bull Seismol Soc Am 1963;53:225–307.
[2] Hanson RD. Behavior of storages tanks, the Great Alaska earthquake of 1964. In: Proceedings national academy of science, Washington DC, 7. p. 331–9.
[3] Manos GC. Evaluation of the earthquake performance of anchored wine tanks during San Juan Argentina, 1977 earthquake. Earthq Eng Struct Dyn 1991;20:1099–114.
[4] Gates WE. Elevated and ground supported steel storage tanks. In: Leeds DJ, editor. Imperial County, California. Earthq Eng Res Inst, Oakland, CA, October 15 1979.
[5] Niwa A, Clough RW. Buckling of cylindrical liquid storage tanks under earthquake loading. Earthq Eng Struct Dyn 1982;10:107–22.
[6] Manos GC, Clough RW. Tank damage during May 1983 Coalinga earthquake. Earthq Eng Struct Dyn 1985;1:449–66.
[7] Hall JF. Northridge earthquake of January 17, 1994: reconnaissance report. Earthq Spectr; 1995; [supplement C to vol. 11]., Vol. 1.
[8] Rai DC. Elevated tanks in Bhuj, India, earthquake of January 26, 2001: reconnaissance report. Earthq Spectr 2001:279–95 [supplement A to vol. 18].
[9] Cruz FE, Valdivia D. Performance of industrial facilities in the Chilean earthquake of 27 February 2010. Struct Des Tall Spec Build 2011;20:83–101.
[10] Almazán JL, Cerda FA, De la Llera JC, López-García D. Linear isolation of stainless steel legged thin-walled tanks. Eng Struct 2007;29(7):1596–611.
[11] González E, Almazán J, Beltrán J, Herrera R, Sandoval V. Performance of stainless steel winery tanks during the 02/27/2010 Maule Earthquake. Eng Struct 2013;56:1402–18.
[12] Kelly JM. Aseismic base isolation: review and bibliography. Soil Dyn Earthq Eng 1986;5(4):202–16.
[13] Soong TT, Dargush GF. Passive energy dissipation systems in structural engineering. 1st ed. New York: John Wiley & Sons; 1997.
[14] Shrimali MK, Jangid RS. Seismic analysis of base-isolated liquid storage tanks. J Sound Vib 2004;275:59–75.
[15] Cho KH, Kim MK, Lim YM, Cho SY. Seismic response of base-isolated liquid storage tanks considering fluid–structure–soil interaction in time domain. Soil Dyn Earthq Eng 2004;24:839–52.
[16] Maleki A, Ziyaeifar M. Damping enhancement of seismic isolated cylindrical liquid storage tanks using baffles. Eng Struct 2007;29:3227–40.
[17] Maleki A, Ziyaeifar M. Sloshing damping in cylindrical liquid storage tanks with baffles. J Sound Vib 2008;311:372–85.
[18] Pirner M, Urushadze S. Liquid damper for suppressing horizontal and vertical motions—parametric study. J Wind Eng Ind Aerodyn 2007;95:1329–49.
[19] Liu D, Lin P. Three-dimensional liquid sloshing in a tank with baffles. Ocean Eng 2009;36:202–12.
[20] Malhotra PK. Seismic strengthening of liquid-storage tanks with energy-dissipating anchors. J Struct Eng 1998;124(4):405–14.
[21] Curadelli O. Seismic reliability of spherical containers retrofitted by means of energy dissipation devices. Eng Struct 2011;33(9):2662–7.
[22] Ormeño M, Geddes M, Larkin T, Chouw N. Experimental study of slip-friction connectors for controlling the maximum seismic demand on a liquid storage tank. Eng Struct 2015;103:134–46.
[23] Colombo JI, Almazán JL. Seismic reliability of continuously supported steel wine storage tanks retrofitted with energy dissipation devices. Eng Struct 2015;98:201–11.
[24] Güneyisi EM, Gülay A. Seismic fragility assessment of effectiveness of viscous dampers in R/C buildings under scenario earthquakes. Struct Saf 2008;30:461–80.
[25] Ellingwood BR. Earthquake risk assessment of building structures. Reliab Eng Syst Saf 2001;74:251–62.
[26] Choi I, Choun Y, Ahn S, Seo J. Probabilistic seismic risk analysis of CANDU containment structure for near-fault earthquakes. Nucl Eng Design 2008;238:1382–91.
[27] Lin K-Ch, Lin Ch-Ch, Chen J-Y, Chang H-Y. Seismic reliability of steel framed buildings. Struct Saf 2010;32:174–82.
[28] Fabbrocino G, Iervolino I, Orlando F, Salzano E. Quantitative risk analysis of oil storage facilities in seismic areas. J Hazard Mater 2005;123:61–9.
[29] Piluso V, Rizzano G, Tolone I. Seismic reliability assessment of a two-story steel-concrete composite frame designed according to Eurocode 8. Struct Saf 2009;31:383–95.
[30] Morgan TA, Mahin SA. Achieving reliable seismic performance enhancement using multi-stage friction pendulum isolators. Earthq Eng Struct Dyn 2010;39(13):1443–61.
[31] Castaldo P, Palazzo B, Della Vecchia P. Seismic reliability of base-isolated structures with friction pendulum bearings. Eng Struct 2015;95:80–93.
[32] Veletsos AS, Tang Y. Soil-structure interaction effects for laterally excited liquid storage tanks. Earthq Eng Struct Dyn 1990;4:473–96.
[33] Constantinou M, Mokha A, Reinhorn A. Teflon bearings in base isolation II: Modeling. J Struct Eng 1990;116:455–74.
[34] Veletsos AS, Shivakumar P, Tang Y, Tang HT. Seismic Response of Anchored Steel Tanks. Proc, 3rd Symposium on Current Issues Related to Nuclear Power Plant Struct., Equip., and Piping, A. J. Gupta, ed., North Caroline State Univ., N. C., 1990; 2–15.
[35] Chalhoub MS, Kelly JM. Theoretical and experimental studies of cylindrical water tanks in base isolated structures. Earthquake Engineering Research Center, University of California at Berkeley; 1988.
[36] MATLAB. High-performance language software for technical computing. Natick (MA): The MathWorks Inc; 2002.
[37] NCH INN NCh 2369 Of 2003. Earthquake resistant design of industrial structures and facilities. Santiago (Chile): Instituto Nacional de Normalización; 2003.
[38] Clough RW, Penzien J. Dynamics of structures. Blue Ridge: McGraw-Hil Inc; 1975.
[39] Dimova SL, Elenas A. Seismic intensity parameters for fragility analysis of structures with energy dissipating devices. Struct Saf 2002;24:1–28.
[40] Murotsu Y, Okada H, Shao S. Reliability-based design of transmission line structures under extreme wind loads. In: Schüeller GI, Shinozuka M, Yao JTP, editors. Structural safety and reliability. ICOSSAR; 1993. p. 1675–81.
[41] Park Y, Ang A, Wen YK. Seismic damage analysis of reinforced concrete buildings. J Struct Eng 1985;111:740–57.
[42] Esteva L, Ruiz SE. Seismic failure rates of multistory frames. J Struct Eng 1989;115:268–84.
[43] Esteva L, Díaz-López O, García-Pérez J. Reliability functions for earthquake resistant design. Reliab Eng Syst Saf 2001;73:239–62.
[44] Neves RA, Mohamed-Chateauneuf A, Venturini WS. Component and system reliability analysis of nonlinear reinforced concrete grids with multiple failure modes. Struct Saf 2008;30:183–99.
[45] Ashraf M, Gardner L, Nethercot DA. Structural stainless steel design: resistance based on deformation capacity. J Struct Eng 2008;134:402–11.
[46] Ellingwood B. Validation studies for seismic PRAs. Nucl Eng Design 1990;123:189–96.
[47] Singhal A, Kiremidjian AS. Method for probabilistic evaluation of seismic structural damage. J Struct Eng 1996;122:1459–67.
[48] Song J, Ellingwood BR. Seismic reliability of special moment steel frames with welded connections: I and II. J Struct Eng 1999;125:357–84.
[49] Ellingwood BR, Kinali K. Quantifying and communicating uncertainty in seismic risk assessment. Struct Saf 2009;31:179–87.
[50] Lee Y, Anderson JG, Zeng Y. Evaluation of empirical ground motion relations in Southern California. Bull Seism Soc Am 2000;90(6B).
[51] Field EH. Accounting for site effects in probabilistic seismic hazard analysis of southern California. Overview of the SCEC phase III report. Bull Seism Soc Am 2000;90(6B). http://www.scec.org/phase3/index.html, http://www.scec.org/resources/catalog/seismichazards.html.
[52] SSHAC (Senior Seismic Hazard Analysis Committee). Recommendations for probabilistic seismic hazard analysis: guidance on uncertainty and use of experts. Washington DC: US Nuclear Regulatory Commission Report CR-6372; 1997.
[53] McGuire RK. Hazard and risk analysis. 1st ed. Oakland (CA): Earthquake Engineering Research Institute; 2004.
[54] Cornell CA, Jalayer F, Hamburger RO, Foutch DA. Probabilistic basis for 2000 SAC FEMA steel moment frame guidelines. J Struct Eng ASCE 2002;128(4):526–33.
[55] BSSC. NEHRP recommended provisions for the development of seismic regulations for new buildings. FEMA report 302. Washington, DC: Federal Emergency Management Agency; 1998.
[56] Kinali K, Ellingwood BR. Seismic fragility assessment of steel frames for consequence-based engineering: a case study for Memphis, TN. Eng Struct 2007;29(6):1115–27.